Dyes and Pigments 99 (2013) 1–5

Contents lists available at SciVerse ScienceDirect

Dyes and Pigments

journal homepage: www.elsevier.com/locate/dyepig

A turn-on fluorescent sensor for Zn(II) based on fluorescein-coumarin conjugate

Jun-mei An, Mi-hui Yan, Zheng-yin Yang*, Tian-rong Li, Qiao-xia Zhou

College of Chemistry and Chemical Engineering, State Key Laboratory of Applied Organic Chemistry, Lanzhou University, No. 222, South Tianshui Road, Lanzhou 730000, PR China

ARTICLE INFO

Article history:
Received 7 January 2013
Received in revised form
11 April 2013
Accepted 15 April 2013
Available online 24 April 2013

Keywords:
Fluorescence chemosensor
Zn^{2+}
Coumarin
Fluorescein
HEPES buffer
Detection limit

ABSTRACT

A novel fluorescent sensor, 7-hydroxy-4-methylcoumarin-8-carbaldehyde-(fluorescein) hydrazone was designed and synthesized for selective recognition of Zn^{2+} in HEPES buffer medium of PH 7.4. This reagent could be used as a probe for Zn^{2+} by monitoring changes in the absorption and the fluorescence spectral patterns. More importantly, this sensor displays an extreme selectivity, sensitivity and color change for Zn^{2+} over other earth- and transition metal ions, which was mainly due to the spirolactam ring-opening power of Zn^{2+}. Upon the addition of Zn^{2+}, an overall emission change of 33-fold was observed and the detection limit was low as 6.54 ppb. Photoinduced electron transfer process, coupled with the intramolecular charge transfer process, are proposed to explain the observed spectral response.

1. Introduction

Zinc is the second most abundant transition metal in the human body behind iron [1], total zinc levels of ~2–3 g in adult, the concentration of Zn^{2+} that is released during neurotransmission is ~300 μM [2]. Zinc plays vital roles in enzyme regulation structure and function, neural signal transmission, and gene expression [3]. Furthermore, Zn^{2+} is mostly trapped within proteins, as a structural or catalytic cofactor [4]. It is also associated with pathological processes, such as Alzheimer's disease, infantile diarrhoea, and cerebral ischemia [5–9]. Accordingly, the development of methods, enabling professionals to spatially and temporally track intracellular Zn^{2+}, is challenging but essential to address these issues and has become the subject of current chemical research.

In comparison with the laborious and expensive traditional detection methods, fluorescent sensor molecules offer useful information about chelatable Zn^{2+} in cellular systems, because we can study the concentration or distribution of Zn^{2+} in real time [10], and fluorescence imaging of Zn^{2+} has become a widely and frequently used technique. Up to now, significant advances have been made in the design of fluorescence probes for Zn^{2+} [11–15]. Most of them, however, have disadvantages such as insufficient selectivity or sensitivity, or interference problems from other transition metal ions, especially Cd^{2+}, which is in the same group of the periodic table and shows similar properties to Zn^{2+} [16–18]. Furthermore, some of them often require laborious multistep organic synthesis [19]. In this sense, the design and synthesis of fluorescent select Zn^{2+} sensors have aroused many scientists' interests.

To develop a simple, facile and reliable Zn^{2+} sensor with better sensitivity, selectivity and solubility, we describe herein a simple Zn^{2+} sensor with functionalized fluorescein-coumarin conjugation. Lippard and collaborators [20–23], Tsien [22], O'Halloran [24,25], Kennedy [26,27], and Gee [28,29], and co-workers have recently introduced a new generation of sensors based on fluorescein chromophores conjugated to picolylamines, aminocarboxylate, and cyclen chelating groups. Although fluorescein derivatives are among the most widely studied and used fluorescent dyes, very few investigations have been carried out on their coumarin conjugates [30]. Coumarins (2H[1]benzopyran-2-ones) have many advantages including high fluorescence quantum yield, large Stokes shift, excellent light stability, and less toxicity. Therefore coumarins have been widely used in the fields of biology, medicine, perfumes, cosmetics, and fluorescent dyes [31–33]. Variations of the nature of the chelating unit, position of the attachment point of the chelating unit (3- or 4-position), and nature of the 7-substituent (−OH, −OAc,

* Corresponding author. Tel.: +86 931 8913515; fax: +86 931 8912582.
E-mail addresses: yangzy@lzu.edu.cn, anjm11@lzu.edu.cn (Z.-y. Yang).

0143-7208/$ – see front matter © 2013 Elsevier Ltd. All rights reserved.
http://dx.doi.org/10.1016/j.dyepig.2013.04.018

or $-NR_2$) on the coumarin play a crucial role in whether, and to what extent, a CHEF-type or ratiometric response of the chemosensor is observed [32]. Herein, we introduced a Schiff base fluorescent sensor 7-hydroxy-4-methylcoumarin-8-carbaldehyde-(fluorescein) hydrazone (**1**) for Zn^{2+}, as shown in Scheme 1.

2. Experimental

2.1. Materials and instrumentation

All solvents and reagents were obtained from commercial suppliers and used without further purification. ^{1}H NMR spectra were measured on a Bruker Avance Drx 300-MHz spectrometer with TMS as an internal standard. ESI-MS were determined on a Bruker esquire 6000 spectrometer. UV–vis absorption spectra were recorded on a Perkin Elmer Lambda 35 UV–vis spectrophotometer. Fluorescence spectra were generated on a Hitachi RF-5301 spectrophotometer equipped with quartz cuvettes of 1 cm path length. Elemental analyses were carried out on an Elemental Vario EL analyzer. IR spectra were obtained in KBr discs on a Thermo Mattson FTIR spectrometer in the 4000–400 cm^{-1} region. The melting points of the compounds were determined on a Beijing XT4-100× microscopic melting point apparatus.

2.2. Synthesis

8-formyl-7-hydroyl-4-methylcoumarin [34] and fluorescein [35] were prepared following the literature method.

In a 250 mL three-necked round bottom flask, 8-formyl-7-hydroyl-4-methylcoumarin (a) (0.245 g, 1.2 mmol) was dissolved in hot ethanol (35 mL) and heated to reflux in an oil bath. Then, a solution of fluorescein hydrazide (b) (0.360 g, 1 mmol) in ethanol (80 mL) was added dropwise to the flask in 1 h, mixture was heated under reflux for 12 h. Finally the white precipitate produced was filtered, dried, and obtained with a yield of 83.8% (0.446 g). The crude product was purified by recrystallization from N,N-dimethylformamide (DMF) to give 0.255 g of **1** as a white solid (57.3%, m.p. > 300 °C). ^{1}H NMR (300 MHz, $CDCl_3$), δ (ppm): 2.35 (s, 3H, CH_3), 6.21 (s, 1H), 6.52(m, 1H), 6.66 (s, 2H), 6.84(m, 1H), 7.19 (m, 1H), 7.66(m, 3H), 7.98(m, 1H), 9.63(s, 1H), 9.99(d, 2H, J = 13 Hz). ^{13}C NMR (300 MHz, $CDCl_3$): 163.61, 160.60, 158.67, 158.17, 153.34, 152.31, 150.38, 146.02, 134.54, 129.36, 128.28, 123.98, 123.41, 113.22, 112.79, 111.86, 110.80, 109.93, 108.63, 105.22, 102.43, 65.36, 56.00, 18.41. ESI-MS: m/z 533.3 $(M + H)^+$. IR (KBr) cm^{-1}: $\nu_{C=O\ (Amide)}$:1726, $\nu_{(Schiff\text{-}base)\ C=N}$:1644. Elemental Analysis (Calcd. for $C_{31}H_{20}N_2O_7$): C, 69.85 (69.92); H, 3.76 (3.79); N, 5.25 (5.26).

2.3. Analysis

Stock solutions (1 mM) of **1** and the nitrate salts (Na^+, K^+, Ca^{2+}, Mg^{2+}, Zn^{2+}, Cu^{2+}, Co^{2+}, Ni^{2+}, Fe^{3+}, Hg^{2+}, Cr^{3+}, Cd^{2+}) were prepared in ethanol. Test solutions were prepared by placing 20 μL of the probe stock solution into cuvettes, adding an appropriate aliquot of each ions stock, and diluting the solution to 2 mL with HEPES buffer (water/ethanol, 1:9, v/v; 10 mM HEPES; pH = 7.4). Both the excitation and emission slit width were 3.0 nm.

3. Results and discussion

In the present study, we have carefully chosen rhodamine and coumarin derivative as the fluorophores in synthesizing the receptor molecule **1**. Details about the synthesis of **1** is discussed above and its characterization data are presented in the supporting information.

3.1. Spectral studies

The changes of the UV–vis spectra for **1** with the gradual addition of Zn^{2+} in HEPES buffer (water/ethanol, 1:9, v/v; 10 mM HEPES; pH = 7.4) were first investigated (Fig. 1). It can be seen from

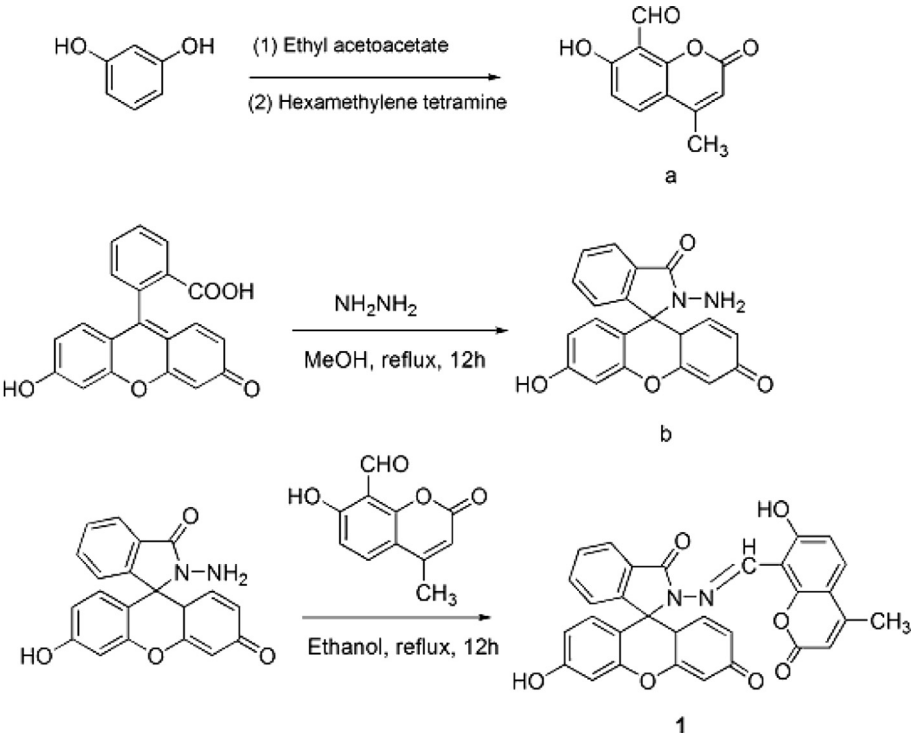

Scheme 1. Synthesis of **1** and reference compounds.

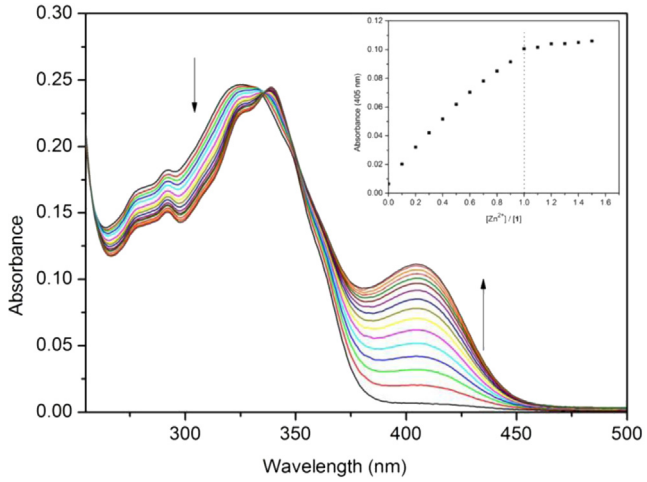

Fig. 1. UV–vis absorption spectra of **1** (10.0 μM) obtained during the titration by $Zn(NO_3)_2$ (0–15.0 μM) in HEPES buffer at room temperature. Inset is the titration profile according to the absorbance at 405 nm.

the curve in Fig. 1 that the free **1** shows a maximum absorption wavelength at 323 nm with a strong absorption intensity. Moreover, free **1** shows almost no characteristic absorption of the fluorescein moiety, demonstrating its existence in the spirolactam form. However, when Zn^{2+} was introduced in the buffered sensing system, the absorbance band at about 323 nm was gradually decreased in intensity, while a new peak appeared at 405 nm and its absorption intensity was increased with the increase of the Zn^{2+} concentration. The new peak at 405 nm belongs to the absorption of the fluorescein moiety. The clearly isosbestic point at 335 nm indicated the formation of a stable **1**-Zn^{2+} complex. This confirms that the addition of Zn^{2+} ions can promote the formation of the ring-opened amide form of compound **1** from spirolactam form. Also, the absorbance based on the band at 405 nm ascends linearly as a function of Zn^{2+} ion concentration and it was saturation at the ratio of 1:1 (inset of Fig. 1). Higher $[Zn^{2+}]_{total}$ does not lead to any further evident change, suggesting a 1:1 stoichiometry for the zinc complex.

Fig. 2 shows the fluorescence spectra of **1** exposed to HEPES buffer (water/ethanol, 1:9, v/v; 10 mM HEPES; pH = 7.4) containing

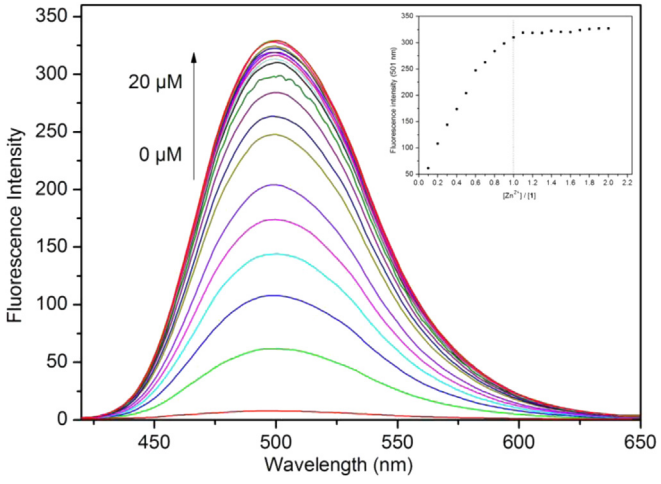

Fig. 2. Fluorescence spectra of **1** (10.0 μM) in HEPES buffer in the presence of different concentrations of Zn^{2+} (0–20 μM) (λ_{ex} = 404 nm, λ_{em} = 501 nm, excitation and emission slit 3 nm). Inset: Fluorescence intensity at 501 nm *vs* concentration of Zn^{2+}.

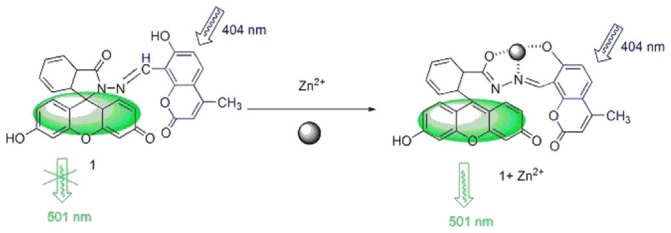

Scheme 2. Chemical structure of the complex and potential binding sites.

different concentration of Zn^{2+} (0–2.0 equiv) recorded at an excitation wavelength of 404 nm and emission wavelength of 420–650 nm. Upon addition of Zn^{2+}, the fluorescence emission intensity of the dosimeter at λ_{ex} = 404nn, λ_{em} = 501 nm was increased 33-fold and was saturated at 1.0 equiv of Zn^{2+}. The remarkable fluorescence enhancement at 501 nm belongs to the fluorescein moiety. So, it can be presumed that Zn^{2+} leads to spirocycle opening of **1** via coordination as shown in Scheme 2.

The detection limit of compound **1** as fluorescence sensor for analysis of Zn^{2+} ions was found to be 6.54 ppb (Fig. S1), which indicate that **1** was highly sensitive to Zn^{2+}. Fluorescence quantum yield measurements were carried out for the sensor to understand its fluorescence behavior observed. The fluorescence quantum yield (φ) of compound **1** in the free and Zn^{2+}-bound state was found to be 0.03 and 0.28, respectively.

3.2. Application value studies

Selectivity is a very important parameter to evaluate the performance of a new fluorescent probe. A highly selective response to the target over other potentially competing species is a necessity. Therefore, the selectivity experiments for probe **1** were extended to various metal ions, such as Na^+, K^+, Ca^{2+}, Mg^{2+}, Cu^{2+}, Co^{2+}, Ni^{2+}, Fe^{3+}, Hg^{2+}, Cr^{3+}, Cd^{2+}. As shown in Fig. 3, a clear fluorescence enhancement (33-fold) is observed with addition of Zn^{2+}, but little fluorescence intensity changes were observed with the above mentioned ions, indicating it has solved well the problem of serious interference from Cd^{2+} met by previous reported typical Zn^{2+} fluorescent probes [36]. Furthermore, the competition experiments

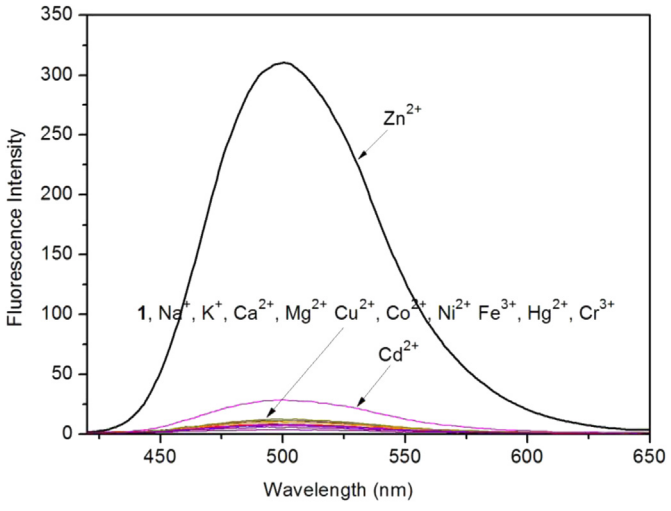

Fig. 3. Fluorescence emission spectra of **1** (10.0 μM) in the presence of different ions, such as Na^+, K^+, Ca^{2+}, Mg^{2+}, Cu^{2+}, Co^{2+}, Ni^{2+}, Fe^{3+}, Hg^{2+}, Cr^{3+}, Cd^{2+} (100.0 μM) and Zn^{2+} (10.0 μM). The excitation was at 404 nm, and the emission was at 501 nm, excitation and emission slit 3 nm.

of Zn^{2+} mixed with the above-mentioned metal ions show that no significant variation is observed in fluorescence intensity (Fig. 4a and Fig. 4b). These facts were indicative of a high selectivity of **1** toward Zn^{2+} over other competitive metal ions. According to the similar binding sites of the reported fluorescent chemosensor [37,38], the high selectivity and competitive for Zn^{2+} of the probe ascribed to the chemical structure of **1** containing oxygen, nitrogen atoms in a special arrangements (Scheme 2).

Reversibility is a prerequisite in developing novel chemosensors for practical application. To test if the proposed complex could be reversed, we carried out a reversibility experiment [37]. The addition of Na_2EDTA to the solution of **1**-Zn^{2+} complexes resulted in gradually quenching of the fluorescence intensity at 501 nm (Fig. S2). The quenching of fluorescence is due to the strong affinity of Na_2EDTA for the Zn^{2+}, which resulted in decomplexation of the receptor-Zn^{2+} complex [39]. These results demonstrate that the Zn^{2+} binding of **1** is chemically reversible, which benefits for the dynamic monitoring of the concentration change of Zn^{2+} in various samples.

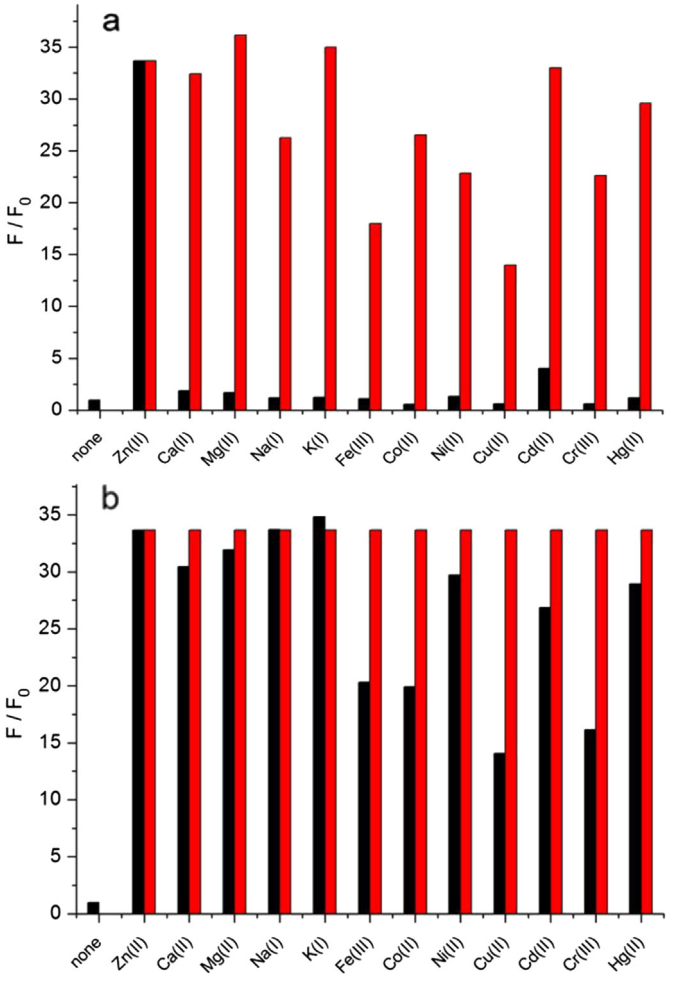

Fig. 4. (a) Selectivity of **1** for Zn^{2+} in the presence of other metal ions in HEPES buffer, the response is normalized with respect to the background fluorescence of the free ligand (F_0). Black bars respect to the addition of an excess of the appropriate metal ion (100.0 μM for Ca^{2+}, Mg^{2+}, Na^+, K^+, Fe^{3+}, Co^{2+}, Ni^{2+}, Cu^{2+}, Cd^{2+}, Cr^{3+}, and Hg^{2+}) to a 10.0 μM solution of **1**; red bars represent the subsequent addition of 10.0 μM Zn^{2+} to the solution. (b) The fluorescence responses of **1** containing Zn^{2+} to different metal ions in HEPES buffer. Red bars, [**1**] = 10.0 μM, [Zn^{2+}] = 10.0 μM; black bars, [**1**] = 10.0 μM, [Zn^{2+}] = 10.0 μM, [M^{n+}] = 100.0 μM. λ_{ex} = 404 nm, λ_{em} = 501 nm, excitation and emission slit 3 nm. (For interpretation of the references to color in this figure legend, the reader is referred to the web version of this article.)

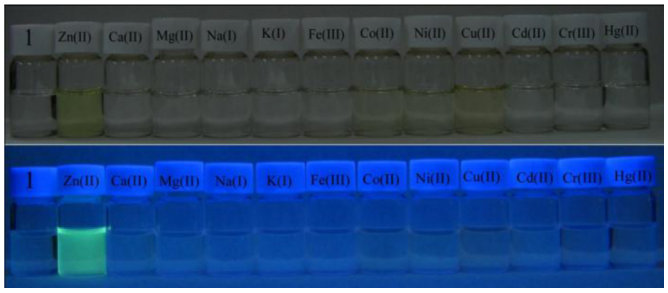

Fig. 5. Color changes of **1** (10.0 μM) upon addition of Zn^{2+} (10.0 μM) and other metal ions (100.0 μM) in HEPES buffer. (For interpretation of the references to color in this figure legend, the reader is referred to the web version of this article.)

3.3. Binding properties and Job's plot

In order to understand the metal-binding properties of **1**, the association constant (K_a) of **1** for Zn^{2+} was calculated to be 1.213×10^4 mol^{-1} from the Scatchard equation [40], which unambiguously demonstrates the strong binding ability of **1** with Zn^{2+} (Fig. S3). The binding ratio is determined to be 0.972, which suggests that **1** should form 1:1 complex in solution with Zn^{2+}. Moreover, **1** can detect Zn^{2+} in visual, and the visible color change can be easily observed by the addition of Zn^{2+}. The sensing ability of fluorescence sensor **1** was tested by mixing it with the metal ions, and only Zn^{2+} caused a visible color change from colorless to light yellow and a green emission (Fig. 5).

To determine the stoichiometry of the **1**-Zn^{2+} complex further, Job's method was applied. The fluorescence emission was measured for each sample by exciting at 404 nm, and then the fluorescence intensity of **1** in the absence (I_0) and presence (I) of Zn^{2+} were determined respectively. A plot of ΔI ($\Delta I = I - I_0$) versus X_M shows that the value goes through a maximum at molar fraction of about 0.5 (Fig. S4), indicating a 1:1 stoichiometry complex formation exactly. This 1:1 stoichiometry was further confirmed from results of the **ESI-MS** data with a peak of [**1** + Zn]$^+$ at m/z 598.3 (Fig. S5).

3.4. ^{13}C NMR and IR spectra

The coordination site of **1** for chelation with Zn^{2+} was confirmed by ^{13}C NMR and IR spectra (Fig. S6 and Fig. S7). Disappearance of ^{13}C NMR signal at 65.65 ppm for tertiary carbon of the spirolactam ring of **1** upon addition of Zn^{2+} confirmed the opening of the spirolactam ring and coordination through $O_{>CO}$ of the fluorescein moiety (Fig. S6) [41]. The infrared spectrum of **1** revealed that the peak at 1726 cm^{-1}, the characteristic frequency for the $C{=}O_{Amide}$ bond of the fluorescein unit, shifted to 1671 cm^{-1} on coordination to the Zn^{2+} ions, in presence of 1.0 equiv of the metal ion (Fig. S7). Such shift in the stretching frequency of $C{=}O_{Amide}$ bond of the rhodamine unit on binding to a metal ion is reported earlier [41]. This appreciable shift support the coordination of the $O_{>CO}$ of the fluorescein unit to Zn^{2+}.

According to ^{13}C NMR and IR spectra, the possible binding mode for **1** to Zn^{2+} is suggested in Scheme 2.

4. Conclusion

In conclusion, a novel fluorescence sensor was prepared by combining two well-know fluorophores, coumarin and fluorescein. The fluorescent sensor (**1**) for Zn^{2+} has a high sensitivity, selectivity and good water-solubility. **1** shows a 33-fold fluorescence enhancement in the presence of Zn^{2+}, and is not significantly

affected by the presence of common physiologically and environmentally important earth- and transition metal ions. From this, we believe that the fluorescence sensor (**1**) has potential application in environmental, biological and medical areas.

Acknowledgments

This work is supported by the National Natural Science Foundation of China (220975046, 81171337 and J1103307).

Appendix A. Supplementary data

Supplementary data related to this article can be found at http://dx.doi.org/10.1016/j.dyepig.2013.04.018.

References

[1] Silva JD, Williams R. The biological chemistry of the elements. Oxford University Press; 2001.
[2] Bush AI. Metals and neuroscience. Curr Opin Chem Biol 2000;4(2):184–91.
[3] Vallee BL, Falchuk KH. The biochemical basis of zinc physiology. Physiol Rev 1993;73:79–118.
[4] Frederickson CJ. Neurobiology of zinc and zinc-containing neurons. Int Rev Neurobiol 1989;31:145–238.
[5] Cuajungco MP, Lees GJ. Zinc metabolism in the brain: relevance to human neurodegenerative disorders. Neurobiol Dis 1997;4:137–69.
[6] Choi DW, Koh JY. Zinc and brain injury. Annu Rev Neurosci 1998;21:347–75.
[7] Weiss JH, Sensi SL, Koh JK. A novel ionic mediator of neural injury in brain disease. Trends Pharmacol Sci 2000;21:395–401.
[8] Suh SW, Jensen KB, Jensen MS, Silva DS, Kesslak PJ, Danscher G, et al. Importance of zinc in the central nervous system: the zinc-containing neuron. Brain Res 2000;852:274–8.
[9] Bush AI. Copper, zinc, and the metallobiology of Alzheimer disease. Alzheimer Dis Assoc Disord 2003;17:147–50.
[10] Mason WT. Fluorescent and luminescent probes for biological activity. 2nd ed. New York: Academic Press; 1999.
[11] Kimura E, Koike T. Recent development of zinc-fluorophores. Chem Soc Rev 1998;27:179–84.
[12] Jiang P, Guo Z. Fluorescent detection of zinc in biological systems: recent development on the design of chemosensors and biosensors. Coord Chem Rev 2004;24:205–29.
[13] Lim NC, Freake HC, Bruckner C. Illuminating zinc in biological systems. Chem Eur J 2005;11:38–49.
[14] Liu ZC, Wang BD, Yang ZY, Li TR, Li Y. A novel fluorescent chemosensor for Zn(II) based on 1,2-(2′-oxoquinoline-3′-yl-methylideneimino)ethane. Inorg Chem Commun 2010;13:606–8.
[15] Yan MH, Li TR, Yang ZY. A novel coumarin Schiff-base as a Zn(II) ion fluorescent sensor. Inorg Chem Commun 2011;14:463–5.
[16] Nolan EM, Lippard SJ. The zinspy family of fluorescent zinc sensors: syntheses and spectroscopic investigations. Inorg Chem 2004;43:8310–7.
[17] Aoki S, Kagata D, Shiro M, Takeda K, Kimura E. Metal chelation-controlled twisted intramolecular charge transfer and its application to fluorescent sensing of metal ions and anions. J Am Chem Soc 2004;126:13377–90.
[18] Parkesh R, Lee TC, Gunnlaugsson T. Highly selective 4-amino-1,8-naphthalimide based fluorescent photoinduced electron transfer (PET) chemosensors for Zn(II) under physiological pH conditions. Org Biomol Chem 2007;5:310–7.
[19] Walkup GK, Burdette SC, Lippard SJ, Tsien RY. A new cell-permeable fluorescent probe for Zn^{2+}. J Am Chem Soc 2000;122:5644–5.
[20] Woodroofe CC, Masalha R, Barnes KR, Frederickson CJ, Lippard SJ. Membrane-permeable and -impermeable sensors of the zinpyr family and their application to imaging of hippocampal zinc in vivo. Chem Biol 2004;11:1659–66.
[21] Burdette SC, Burdette GK, Springler B, Tsien RY, Lippard SJ. Fluorescent sensors for Zn^{2+} based on a fluorescein platform: synthesis, properties and intracellular distribution. J Am Chem Soc 2001;123:7831–41.
[22] Burdette SC, Frederickson CJ, Bu W, Lippard SJ. ZP4, an improved neuronal Zn^{2+} sensor of the zinpyr family. J Am Chem Soc 2003;125:1778–87.
[23] Clark MA, Duffy K, Timbrewala J, Lippard SJ. Synthesis and metal-binding properties of chelating fluorescein derivatives. Org Lett 2003;5:2051–4.
[24] Nasir MS, Fahrni CJ, Suhy DA, Kolodsick KJ, Singer CP, O'Halloran TV. The chemical cell biology of zinc: structure and intracellular fluorescence of a zinc-quinolinesulfonamide complex. J Biol Inorg Chem 1999;4:775–83.
[25] Taki M, Wolford JL, O'Halloran TV. Emission ratiometric imaging of intracellular zinc: design of a benzoxazole fluorescent sensor and its application in two-photon microscopy. J Am Chem Soc 2004;126:712–3.
[26] Qian WJ, Aspinwall CA, Battiste MA, Kennedy RT. Detection of secretion from single pancreatic β-cells using extracellular fluorogenic reactions and confocal fluorescence microscopy. Anal Chem 2000;70:711–7.
[27] Gee KR, Zhou ZL, Qian WJ, Kennedy R. Detection and imaging of zinc secretion from pancreatic β-cells using a new fluorescent zinc indicator. J Am Chem Soc 2002;124:776–8.
[28] Sensi SL, Ton-That D, Weiss JH, Rothe A, Gee KR. A new mitochondrial fluorescent zinc sensor. Cell Calcium 2003;34:281–4.
[29] Gee KR, Zhou ZL, Ton-That D, Sensi SL, Weiss JH. Measuring zinc in living cells. A new generation of sensitive and selective fluorescent probes. Cell Calcium 2002;31:245–51.
[30] Kim HJ, Park JE, Choi MG, Ahn S, Chang SK. Selective chromogenic and fluorogenic signalling of Hg^{2+} ions using a fluorescein-coumarin conjugate. Dyes Pigm 2010;84:54–8.
[31] Haugland RP. Handbook of fluorescent probes and research products. Eugene, OR: Mol. Cell Probe Inc; 2005.
[32] Katerinopoulos HE. The coumarin moiety as chromophore of fluorescent ion indicators in biological systems. Curr Pharm Des 2004;10:3835–52.
[33] Lim NC, Schuster JV, Porto MC, Tanudra MA, Yao LL, Freake HC, et al. Coumarin-based chemosensors for zinc(II): toward the determination of the design algorithm for CHEF-type and ratiometric probes. Inorg Chem 2005;44:2018–30.
[34] Bender DR, Kanne D, Frazier JD, Rapoport H. Synthesis and derivatization of 8-acetylpsoralens. Acetyl migrations during Claisen rearrangement. J Org Chem 1983;16:2709–19.
[35] Dujols V, Ford F, Czarnik AW. A long-wavelength fluorescent chemodosimeter selective for Cu(II) ion in water. J Am Chem Soc 1997;119(31):7386–7.
[36] Wang LN, Qin WW, Liu WS. A novel coumarin Schiff-base as a Zn(II) ion fluorescent sensor. Inorg Chem Commun 2010;13:1122–5.
[37] Zhou Y, Wang F, Kim Y, Kim SJ, Yoon J. Cu^{2+}-selective ratiometric and "off–on" sensor based on the rhodamine derivative bearing pyrene group. Org Lett 2009;11(19):4442–5.
[38] Saha S, Mahato P, Reddy GU, Suresh E, Chakrabarty A, Baidya M, et al. Recognition of Hg^{2+} and Cr^{3+} in physiological conditions by a rhodamine derivative and its application as a reagent for cell-imaging studies. Inorg Chem 2012;51:336–45.
[39] Schwarzenbach G, Freitag E. Helv Chim Acta 1951;34:1503–8.
[40] Lakowicz JR. Fluorescence quenching: theory and applications, principles of fluorescence spectroscopy. New York: Kluwer Academic/Plenum Publishers; 199953–127.
[41] Lee MH, Wu JS, Lee JW, Jung JH, Kim JS. Highly sensitive and selective chemosensor for Hg^{2+} based on the rhodamine fluorophore. Org Lett 2007;9(13):2501–4.